UNIVERSIDADE DE SANTIAGO DE COMPOSTELA

Centro de Investigación en Química Biolóxica e Materiais Moleculares (CiQUS), **Department of Organic Chemistry**

Double bachelor's degree in Chemistry and Biology

Final Degree Project

Development of New Antipseudomonal Antibiotics Through Irreversible Inhibition of the Enzyme EPSP Synthase

Author: Melisse Bisbé Brito
Supervisor: Concepción González Bello
Course: 2021/2022

Dña. CONCEPCIÓN GONZÁLEZ BELLO, CATEDRÁTICA DE LA UNIVERSIDADE DE SANTIAGO DE COMPOSTELA, INFORMA:

Que la memoria adjunta, titulada "*Development of New Antipseudomonal Antibiotics Through Irreversible Inhibition of the Enzyme EPSP Synthase*", que para optar al título de Doble Grado en Química y Biología presenta Melisse Bisbé Brito, ha sido realizada bajo mi dirección en los laboratorios del Centro Singular de Investigación en Química Biolóxica e Materiais Moleculares (CiQUS) de la Universidade de Santiago de Compostela.

Considerando que constituye trabajo de "Trabajo de Fin de Grado", autoriza su presentación en la Universidade de Santiago de Compostela.

Y, para que así conste, firmo el presente informe en Santiago de Compostela a 4 de Julio de dos mil veintidós.

GONZALEZ BELLO, CONCEPCION (AUTENTICACIÓN)

Firmado digitalmente por GONZALEZ BELLO, CONCEPCION (AUTENTICACIÓN)
Nombre de reconocimiento (DN): c=ES, serialNumber=36072322L, sn=GONZALEZ, givenName=CONCEPCION, cn=GONZALEZ BELLO, CONCEPCION (AUTENTICACIÓN)
Fecha: 2022.07.04 13:17:15 +02'00'

Fdo: Concepción González Bello

ABBREVIATIONS

anh	Anhydrous
Arg	Arginine
ATP	Adenosine triphosphate
ATR	Attenuated total reflectance
(c)	Concentrated
^{13}C-NMR	Carbon-13 nuclear magnetic resonance
δ	Chemical shift
Δ	Reflux
d	Doublet
DAAE	Ethyl diazoacetate
DCM	Dichloromethane
dd	Double doublet
ddt	Triplet double doublets
DEPT	Distortionless Enhancement by Polarization Transfer
DIPEA	*N*,*N*-Diisopropylethylamine
DMAP	4-Dimethylaminopyridine
DMF	*N*,*N*-Dimethylformamide
DNA	Deoxyribonucleic acid
E.	*Escherichia*
EDC	1-Ethyl-3-(3-dimethylaminopropyl)carbodiimide
EPSP	5-enolpyruvylshikimate 3-phosphate
EPSPS	5-enolpyruvylshikimate 3-phosphate synthase
EPSPS-*Ec*	EPSP synthase from *E.* coli
EPSPS-*Mt*	EPSP synthase from *M.* tuberculosis
ESI	Electrospray ionization
h	Hours
His	Histidine
^{1}H-NMR	Proton Nuclear magnetic resonance
HRMS	High-resolution mass spectrometry
Hz	Hertz
IR	Infrared
J	Coupling constant

K_i	Inhibitory constant
Lys	Lysine
m	Multiplet
M	Molar
m/z	Mass/charge ratio
M.	*Mycobacterium*
MIC	Minimum inhibitory concentration
M^+	Molecular Ion
MH^+	Molecular ion plus a proton
MNa^+	Molecular ion plus sodium
MD	Molecular Dynamics
MS	Mass spectrometry
NMR	Nuclear magnetic resonance
PDB	Protein Data Bank
PEP	Phosphoenolpyruvate
Phe	Phenylalanine
ppm	Parts per million
Py	Pyridine
q	Quartet
RNA	Ribonucleic acid
rRNA	Ribosomal ribonucleic acid
s	Singlet
rt	Room temperature
Ser	Serine
S3P	Shikimate-3-phosphate
t	Triplet
td	Double triplet
TB	Tuberculosis
THF	Tetrahydrofuran
Trp	Tryptophan
Tyr	Tyrosine
UV	Ultraviolet
WHO	World Health Organization

INDEX

ABSTRACT

The introduction of antibiotics to treat infectious diseases transformed the landscape of medical science. However, the emergence of multidrug-resistant bacteria has been rising, reaching alarming levels worldwide and jeopardizing their value. For this reason, it is urgent to develop novel and alternative therapies by identifying unexplored bacterial targets. This project aims to study the therapeutic potential of EPSP synthase (EPSPS), the sixth enzyme of the shikimic acid metabolic pathway, involved in the biosynthesis of aromatic amino acids and other essential metabolites for bacteria. Irreversible inhibition of this enzyme from the target compound (amide **19**), capable of modulating its reactivity upon binding to the specific target, will be studied. This compound will have a chloroacetamide group as a latent electrophile that will covalently modify the Lys23 residue, located in the active site and essential in the mechanism of action of the enzyme.

RESUMEN

La introducción de los antibióticos para el tratamiento de enfermedades infecciosas supuso una transformación en el panorama de las ciencias médicas. Sin embargo, la aparición de bacterias multirresistentes ha ido en aumento, alcanzando niveles alarmantes en todo el mundo y poniendo en peligro su valor. Por este motivo, es urgente desarrollar terapias novedosas y alternativas, identificando dianas bacterianas inexploradas. Este trabajo pretende estudiar el potencial terapéutico de la EPSP sintasa (EPSPS), la sexta enzima de la ruta metabólica del ácido siquímico, involucrada en la biosíntesis de los aminoácidos aromáticos y otros metabolitos esenciales para las bacterias. Se estudiará la inhibición irreversible de esta enzima a partir del compuesto objetivo (amida **19**), capaz de modular su reactividad al unirse con la diana específica. Este compuesto presentará un grupo cloroacetamida como electrófilo latente que modificará covalentemente el residuo Lys23, ubicado en el centro activo y esencial en el mecanismo de acción de la enzima.

RESUMO

A introdución dos antibióticos para o tratamento de enfermidades infecciosas supuxo unha transformación no panorama das ciencias médicas. Con todo, a aparición de bacterias multirresistentes foi en aumento, alcanzando niveis alarmantes en todo o mundo e poñendo en perigo o valor dos mesmos. Por este motivo, é urxente desenvolver terapias novas e alternativas, identificando dianas bacterianas inexploradas. Este traballo pretende estudar o potencial terapéutico da EPSP sintasa (EPSPS), a sexta enzima da ruta metabólica do ácido siquímico, involucrada na biosíntese dos aminoácidos aromáticos e outros metabolitos esenciais para as bacterias. Estudarase a inhibición irreversible da enzima para partir do composto obxectivo (amida **19**), capaz de modular a súa reactividade ao unirse coa diana específica. Este composto presentará un ligando cun grupo cloroacetamida como electrófilo latente que modificará covalentemente o residuo Lys23, situado no centro activo e esencial no mecanismo de acción da enzima.

1 INTRODUCTION

1.1 Bacterial Resistance to Antibiotics

The introduction of antibiotics almost 50 years ago into clinical practice revolutionized the treatment and management of infectious diseases and has changed the landscape of contemporary medicine. Since the discovery of penicillin in 1942, antibiotics have contributed to reduce global deaths from infectious diseases by over 70%.[1] This success led to the false belief that the war against bacteria was over. However, it was soon discovered that bacteria are able to develop very efficient resistance mechanism to escape from antibiotic action (Figure 1).[2,3]

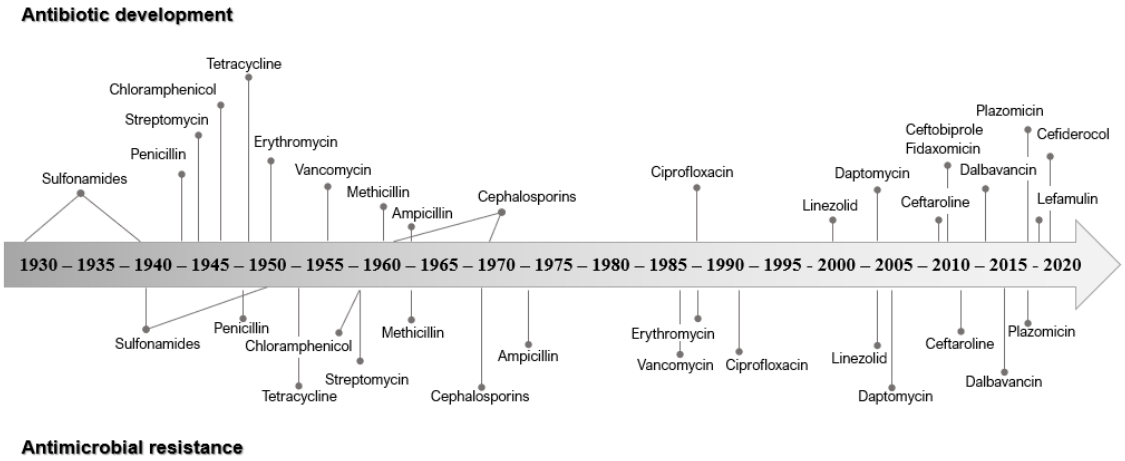

Figure 1*. Comparison over time of the clinical introduction of antibiotics and the emergence of bacterial strains resistant to each antibiotic.*

Despite the recognized need for new antibiotics, only four new classes have been commercialized since the early 1960s.[4] Research was mainly focused on modifying existing ones to increase their efficacy against multidrug-resistant bacteria, however all these efforts have not been enough. The widespread use, misuse, and abuse of antibiotics, not only in the treatment and prevention of bacterial infections in humans but also in veterinary medicine, as growth promoters in animal production and agriculture, have triggered the emergence and spread worldwide of very efficient resistance mechanisms in various bacterial populations.[5]

The World Health Organization (WHO) considers that the emergence of multi-drug resistant pathogens is a public health emergency of unknown proportions for which new antibiotics is urgently needed.[6] Besides this necessity, big pharmaceutical companies

have largely abandoned the antimicrobial research area and as a result, the pipeline for antibiotics is almost empty compared to more than 500 drugs for chronic diseases for which resistance is not an issue.[7,8] If no immediate action is taken, the estimated number of deaths due to antibiotic resistance will rise to 10 million by 2050, exceeding the mortality rate from cancer.[9]

According to the WHO, the most critical group of bacterial pathogens are *Acinetobacter baumannii*, *Pseudomonas aeruginosa* and various Enterobacteriaceae (including *Klebsiella*, *Escherichia coli*, *Serratia* and *Proteus*). All these bacteria are resistant to carbapenems and third generation cephalosporins, which are the best available antibiotics for treating multidrug resistant bacteria.[10] Also relevant is *Mycobacterium tuberculosis*, the causative agent of tuberculosis, which is one of the ten most deadly diseases in the world and a global priority.[8]

Specifically, *Pseudomonas aeruginosa* is one of the most frequent and severe causes of hospital-acquired infections, including pneumonia, bloodstream infections, urinary tract infections, and surgical site infections. This microorganism is associated with high morbidity and mortality, particularly affecting immunocompromised patients or those with chronic debilitating diseases because they cannot respond to conventional treatments. The European Antimicrobial Resistance Surveillance Network of the European Centre for Disease Prevention and Control (ECDC) (EARS-Net) has reported that 32.1% of *Pseudomonas aeruginosa* isolates in the European Union/European Economic Area were resistant to at least one of the antimicrobial groups under regular surveillance and 19.2% of all tested isolates were resistant to two or more antimicrobial groups.[11] The various mechanisms for adaptation, survival, and resistance to multiple classes of antibiotics of this bacterium are why it is a threat to global public health and the treatment options are becoming increasingly limited.

1.2 Therapeutic Targets of Antibiotics

Antibiotics can either be bactericidal, i.e., exert their effect by killing the bacterium, or they can be bacteriostatic, i.e., exert their effect by inhibiting the growth of the bacterium and thus enabling the host's immune system to eliminate the infection.[12] There are currently five main targets for antibiotics: (1) cell-wall biosynthesis, in which the antibiotic binds to enzymes involved in the synthesis; (2) protein synthesis, through reversible binding to bacterial 30S and 50S ribosomal subunits; (3) DNA replication and

repair (RNA polymerase, DNA gyrase); (4) folic acid metabolism, by inhibiting a specific enzyme called dihydropteroate synthase (DHPS); and (5) membrane structure.[13]

1.3 Mechanisms of Antimicrobial Resistance

Bacterial resistance is a natural process due to the evolution and adaptability inherent in bacteria.[8] Nevertheless, human behavior has undoubtedly been instrumental in bringing bacterial resistance to its current alarming level. In addition to the mutation of various genes on the chromosomes of the microorganisms, the exchange of genetic material between organisms plays a crucial role in the spread of antibiotic resistance.[14] The horizontal gene transfer could happen through three different mechanisms:[15] (1) transformation, in which the bacterium captures DNA from the environment; (2) transduction, via bacteriophages and (3) conjugation, by plasmids that contain resistance genes, which is the most important phenomenon. Antibiotics can enhance this process by inducing the transfer of resistance elements or by exerting selection pressure on the emergence of resistance.

There are four main resistance mechanisms to antibiotics:[8] (1) modifications of the drug target, which decreases the affinity for the antibiotic; (2) changes in the outer membrane permeability, limiting the uptake of a drug; (3) drug excretion by activation of efflux pumps; and (4) enzymatic inactivation of the antibiotic, in such a way that it no longer affects the microorganism (Figure 2). The last mechanism is the most common cause of antibiotic resistance in Gram-negative bacteria and the most relevant example is the enzyme-catalyzed hydrolysis of β-lactam antibiotics by β-lactamase enzymes.

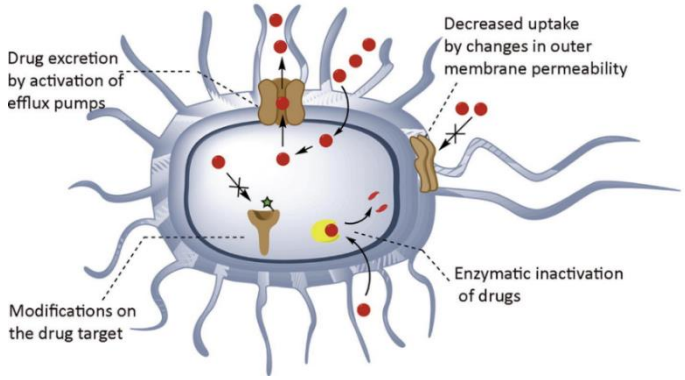

Figure 2.[8] *Representation of the main mechanisms of bacterial resistance.*

Antibiotic discovery is hindered by several intrinsic factors. For example, the permeability barrier formed by the outer membrane of Gram-negative prevents antibiotics from accessing their targets and that is why they usually are more resistant strains than Gram-positive bacteria.[14] Therefore, treating infections caused by these bacteria by developing antibiotics remains a challenge.[16]

1.4 Therapeutic Strategies to Combat Antibiotic Resistance

Much of the research for new antibiotics is still focused on developing improved versions of existing drugs by targeting a small number and the same type of bacterial targets. However, bacteria have already developed very efficient resistance mechanism to escape from them. Therefore, new drugs targeting unexplored bacterial targets to deal with antibiotic-resistant infections are urgently needed.[17] In recent years, much effort has been devoted to identify genes that are essential for bacterial survival, as well as the enzymes or receptors encoded by them, as a way to identify new niches for drug discovery. In addition, the recent advances in the resolution of numerous three-dimensional crystal structures of various key enzymes/proteins in bacterial metabolism have had a positive impact on the rational development of inhibitors/antagonists of these targets.[18]

1.5 Shikimic Acid Metabolic Pathway

One strategy for obtaining new antibiotics is to develop compounds that can interfere with crucial bacterial metabolic processes. An example of such a process is the shikimic acid metabolic pathway through which seven enzymes catalyze the conversion of phosphoenolpyruvate (**1**) and erythrose-4-phosphate (**2**) to chorismate (**3**) (Scheme 1).[19] The latter compound is the precursor of three aromatic amino acids: phenylalanine, tyrosine, and tryptophan, as well as many aromatic secondary metabolites, including folate cofactors, ubiquinone, and vitamins E and K.[20] This metabolic pathway is found only in plants, bacteria, fungi, and certain apicomplexan parasites,[21] *Plasmodium falciparum* (the causative agent of malaria), *Toxoplasma gondii*, and *Cryptosporidium parvum*, but not in mammals.[22] The fact that the enzymes involved in this metabolic pathway are essential in certain important microorganisms but absent in mammals makes them also attractive targets for the development of antimicrobial agents and herbicides. In particular, the enzymes of this pathway are attractive for anti-TB drug discovery since five of the seven genes coding for the enzymes of the pathway (*aroF*, *aroG*, *aroB*, *aroD*, *aroE*, *aroK* and *aroA*) are essential for *Mycobacterium tuberculosis*.[23]

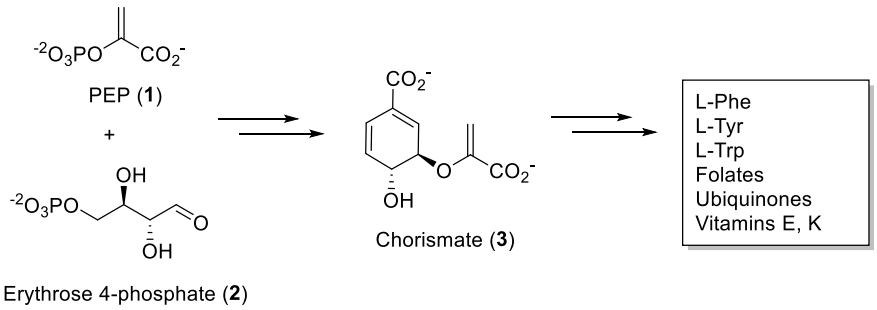

Scheme 1. *Shikimic acid metabolic pathway.*

EPSP Synthase Enzyme

This project is focus on the sixth enzyme of the pathway, 5-enolpyruvylshikimate 3-phosphate (EPSP) synthase. Some of the factors that make this enzyme an attractive therapeutic target are:

(1) The *aroA* gene encoding for EPSP synthase from *Acinetobacter baumannii* is essential *in vivo*.[24] The EPSP synthase enzyme is also essential for *Mycobacterium tuberculosis* and *Klebsiella pneumoniae*.

(2) Deletion of the *aroA* gene that encodes for *Pseudomonas aeruginosa* and *Salmonella typhimurium* produces oral vaccines in mice and calves, respectively, so this enzyme could also act as an *in vivo* virulence factor in these bacteria.[25]

(3) This enzyme does not have any counterpart in humans.

EPSP synthase catalyzes the transfer of the enolpyruvyl moiety from phosphoenolpyruvate (PEP, **1**) to shikimate-3-phosphate (S3P, **4**) to yield 5-enolpyruvylshikimate 3-phosphate (EPSP, **7**) and inorganic phosphate through an addition-elimination reaction (Scheme 2).[26] First, the nucleophilic attack by the 5-hydroxyl group of shikimate-3-phosphate (**4**) to C2 of PEP (**1**) affords a tetrahedral intermediate **5** (THI). Next, this intermediate undergoes an elimination reaction to yield an intermediate carbocation **6**, which subsequent deprotonation reaction affords the final product, EPSP (**7**).[22]

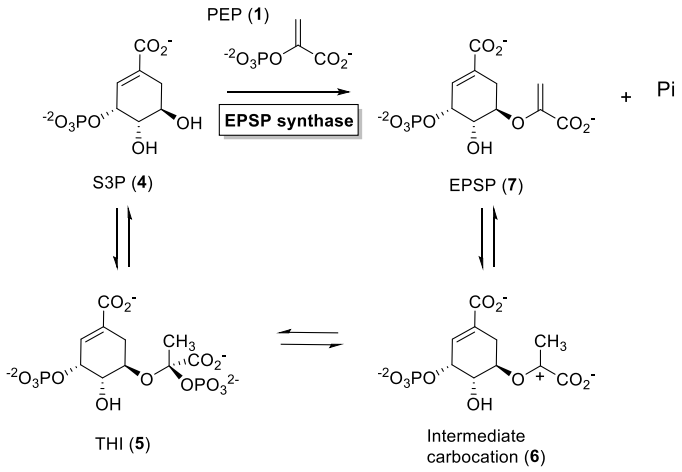

***Scheme 2**. Enzymatic conversion catalyzed by the EPSP synthase enzyme*.

EPSP synthase is a monomeric enzyme with a molecular mass of about 46 kDa. The crystal structure of EPSP synthase from *E.coli* (EPSPS-*Ec*) and *M. tuberculosis* (EPSPS-*Mt*) is available.[26] The structure shows two domains, namely domains 1 and 2, with the active site located near the interdomain crossing segment (Figure 3). Comparison of the wild-type form [open (PDB 2BJB)][27] and the structure in complex with the substrates/products [close (PDB 2O0Z)][28] revealed that domain 1 closes over domain 2 for catalysis.[22] Thus, upon substrate binding, a significant substrate-induced conformational changes occur in domain 1 (> 12 Å), resulting in the closed conformation, which is the active form for catalysis. Shikimate-3-phosphate (**4**) was thought to initially bind to domain 2[29], triggering the folding of domain 1 to the closed conformation, but recent molecular dynamics simulation studies carried out in the research group of Prof. González Bello showed the opposite. Thus, it is phosphoenolpyruvate that triggers the folding of domain 1, creating a small entry channel for S3P (**4**) to tidily seal the active site. This indicates that blocking the recognition center of PEP (**1**) could prevent the formation of the active conformation for catalysis.

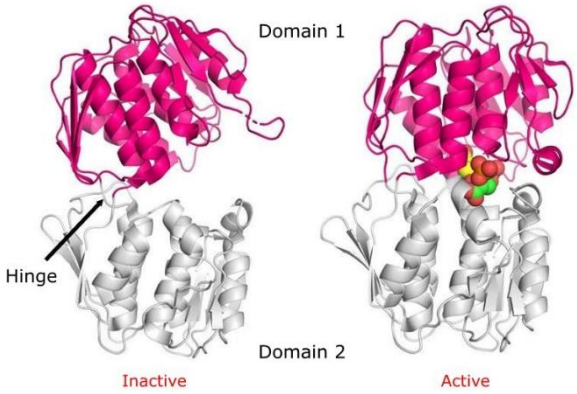

Figure 3. *X-ray crystal structures of EPSPS-Mt enzyme in the open (wild-type, PDB 2BJB, 1.80 Å, left) and closed form (in complex with S3P and FEP, PDB 2O0E, 1.81 Å, right). S3P (**4**) and PEP (**1**) are shown as yellow and green spheres, respectively.*

The analysis of the main interactions observed in PDB 2O0E structure revealed that S3P (**4**) is anchored in the active site through a strong electrostatic interaction between its carboxylate group and the guanidinium group of Arg28, as well as numerous hydrogen bonding interactions with the side chains of residues Ser168, Ser196, His336, and His340 (Figure 4). On the other hand, PEP (**1**) establishes strong electrostatic interactions with the guanidinium groups of residues Arg385 and Arg124, and hydrogen bonding interactions with the terminal amino groups of residues Lys410 and Lys23 (Figure 4). The residue Lys23, which is located near the hinge, is believed to be key for the enzymatic reaction because it would act in the deprotonation of the C5 hydroxyl group in S3P (**4**), facilitating the nucleophilic attack of the latter. Also, it revealed to be involved in the elimination reaction leading to the product.[26]

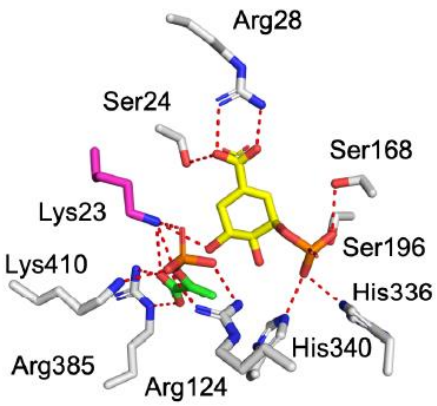

Figure 4*. Detailed view of the main polar contacts of S3P (**4**) and FEP (**1**) in PDB 2O0E. The main electrostatic and hydrogen bonding interactions are shown as red dashed lines. The side chains of relevant residues are shown and labeled. The residue Lys23 is highlighted in pink.*

1.6 EPSP Synthase Inhibitors

N-[phosphonomethyl]glycine (**8**), also known as glyphosate, is the first reported inhibitor of the EPSPS enzyme and the only one commercially available (Scheme 3).[22] This compound is the broad-spectrum active principle of the herbicides Round® and TouchdownPremium®. Glyphosate (**8**) is a competitive reversible inhibitor of the enzyme that competes with PEP (**1**) (K_i= 0.2 μM) for binding.[30] It does not bind to the apo-form but rather to the binary EPSPS@S3P complex. The positive charge on the amino group of the herbicide mimics the developing carbocation characteristics of the natural substrate. The ternary EPSPS@S3P-glyphosate complex has long been considered a mimic of the transition state in which glyphosate takes the place of PEP, but studies have shown that, in spite of the competitive nature, glyphosate and PEP binding are not totally equivalent. For that reason, this inhibition was named an "adventitious allosteric interaction".[22] It appears that the confined space of the active site of EPSP synthase prohibits even slight alterations of the glyphosate molecule. More than 1.000 analogs of glyphosate have been produced and tested for inhibition of EPSP synthase, but they have failed to improve the binding affinity of the parent compound.[31] Glyphosate, which is an organophosphorus compound, showed to be toxic for use in humans.

On the other hand, Alberg and Bartlett developed two stable analogs of the tetrahedral intermediate **5** (Scheme 3).[32] Both diastereomers showed to be good competitive reversible inhibitors. Compound **9** proved to be the most potent with K_i value of 15 nM against EPSP synthase from *Petunia hybrida,* which represents the most potent inhibitor against this enzyme yet reported. This compound proved to be 50-fold more potent than its *S*-isomer **10** (K_i = 750 nM) and has the opposite stereochemistry in the side chain compared with intermediate **5**. Recent crystallographic studies have shown that the presence of the phosphonate group in compound **9** induces substantial conformational changes in the side chains of diverse conserved residues within the enzyme active site that explains its higher potency. On the contrary, compound **10** does not induce conformational changes on the latter residues and the arrangement of the enzyme active site is as for the intermediate **5**.[22] Unfortunately, these inhibitors have the same toxicity problem as glyphosate because they are organophosphates.

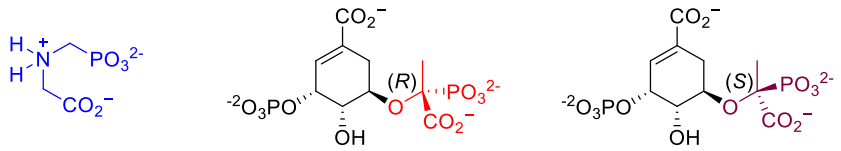

***Scheme 3**. Reported inhibitors of EPSP synthase; glyphosate (**8**), R- (**9**) and S-phosphonate analogs (**10**) of the tetrahedral intermediate.*

More recently, Miller *et al.* developed other type of inhibitors of EPSP synthase, in which the cyclohexane ring was replaced by an aryl group (Scheme 4).[33] The molecular basis of the design was based on flattened conformation adopted by the cyclohexane ring in the substrate and the product for recognition. Among them, compound **11** has been identified as a good inhibitor and several analogs of **11** have also been synthesized. This is the case of **12**, **13**, and **14**, in which the 3-phosphate functionality has been replaced with either a malonate ether group (**12** and **13**) or the shortened hydroxy malonate moiety (**14**). The greater potency of these compounds versus their corresponding phenol analogs **15-17** shows that multiple anionic charges at the dihydroxybenzoate-5 position are required to achieve effective EPSPS inhibition. Some results have suggested that the 3-malonate ether moiety represents a less than ideal solution as a spatial mimic of the more labile 3-phosphate group, that is why the development of aromatic inhibitors incorporating slightly shortened 3-phosphate mimics as the compound **18** has demonstrated to be more effective.[34]

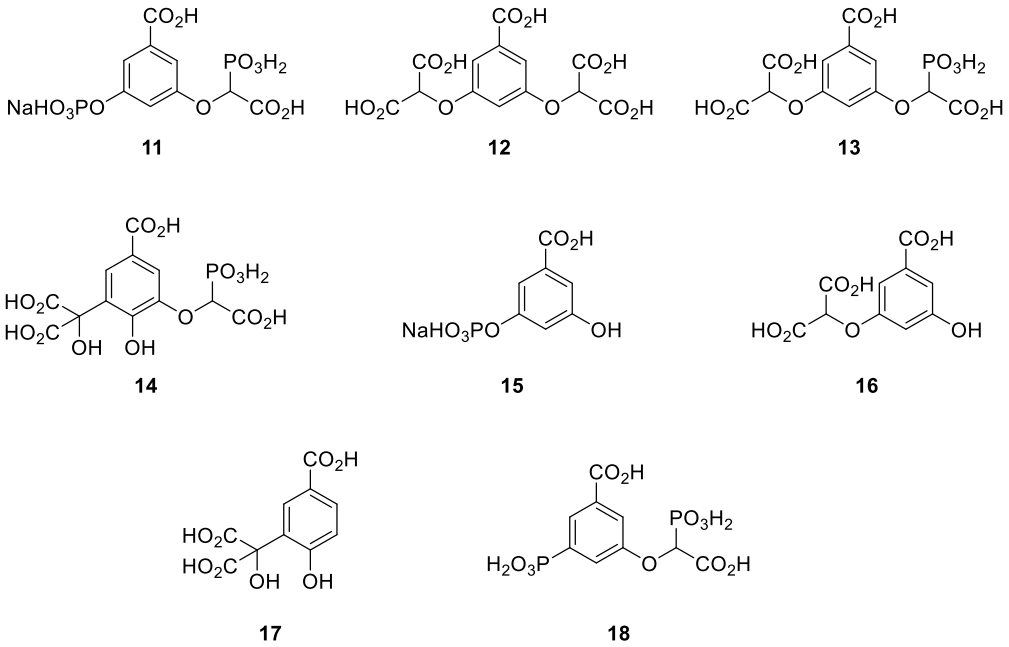

***Scheme 4**. Aromatic achiral inhibitors developed by Miller and collaborators.*

1.6.1 Irreversible Inhibitors

For the discover small-scale drug candidates with attractive toxicity profiles, the pharmaceutical industry has predominantly sought compounds that modulate target proteins through noncovalent interactions.[35] For many years the development of irreversible inhibitors was hindered due to their potential to react with non-target proteins and provoke immune responses.[36] The more detailed knowledge available today on the real risks associated with this type of inhibitors and its huge advantages has led to a dramatic increase in their presence in anti-infective discovery programs. Irreversible inhibitors bind to the target and then react with it by forming a stable covalent adduct that permanently blocks its function (Figure 5). This type of inhibitors have many advantages, such as their increased efficiency and selectivity, prolonged action, and reduced risk of drug resistance due to active site residue changes.[36] Besides these advantages, the design of this kind of ligands remains a challenge due to the need to combine in a single chemical entity, both, reactivity, and selectivity.[37] That is why the design of ligands with high affinity for the selected target and less reactive electrophiles ("latent electrophiles") has become an emerging area in drug development. It is possible to achieve potency without sacrificing selectivity since they would be hidden to non-specific targets and are only activated for the chemical modification reaction upon binding. Most of these ligands have been designed to modify cysteine residues. Targeting lysine residues appears to be more difficult because their ε-amino group is usually not nucleophilic, being protonated at physiological pH.[37] However, over the years, the research group I have worked with has investigated the development of novel irreversible lysine inhibitors capable of modulating their reactivity when complementarity with the specific target takes place and obtained satisfactory results.

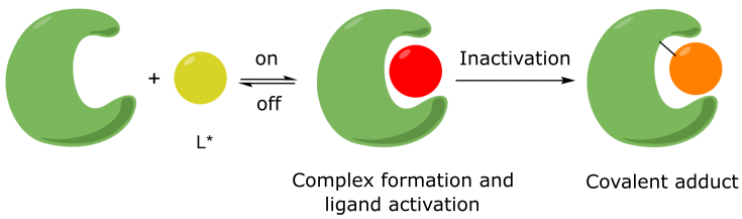

***Figure 5**. Inhibition of a target by binding of an irreversible inhibitor.*

2 OBJECTIVES AND HYPOTHESIS

The general objective of this bachelor's final project is the development of a novel antibiotic with a new mechanism of action to combat the worldwide increasing appearance of multi-drug resistant bacteria based on the inhibition of the EPSP synthase enzyme, an essential enzyme for the survival of *Pseudomonas aeruginosa* and other relevant pathogens. In particular, the goal of this work is the synthesis of a non-toxic and selective irreversible inhibitor, compound **19**, capable to cause a covalent modification of the EPSP synthase (Figure 6).

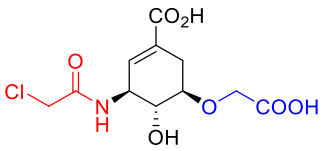

19

***Figure 6**. Target compound **19**.*

The molecular basis and hypothesis for the design of this compound are the following:

(1) The residue Lys23, which showed to be essential for catalysis, has an estimated pKa value of 3.5[38], and therefore it would be neutral at physiological pH and suitable for undergoing reactions as a nucleophile.

(2) Preliminary results in the González-Bello's group showed that compound **20**, which has an activated carbon atom (chloromethyl amido group) is suitable for nucleophilic attack (Figure 7A). This compound showed excellent *in vitro* activity against the virulent strain of *M. tuberculosis* (H37Rv), with a minimum inhibitory concentration (MIC) of 10 μg mL^{-1}.[18] Incubation studies with EPSPS-*Mt* and subsequent proteomic analysis confirmed covalent modification of the enzyme. Furthermore, Molecular Dynamics (MD) simulation studies carried out by the research group also showed that the side-chain of Lys23 would have the suitable arrangement for nucleophilic attack to the aforementioned carbon atom (Figure 7B and 7D).

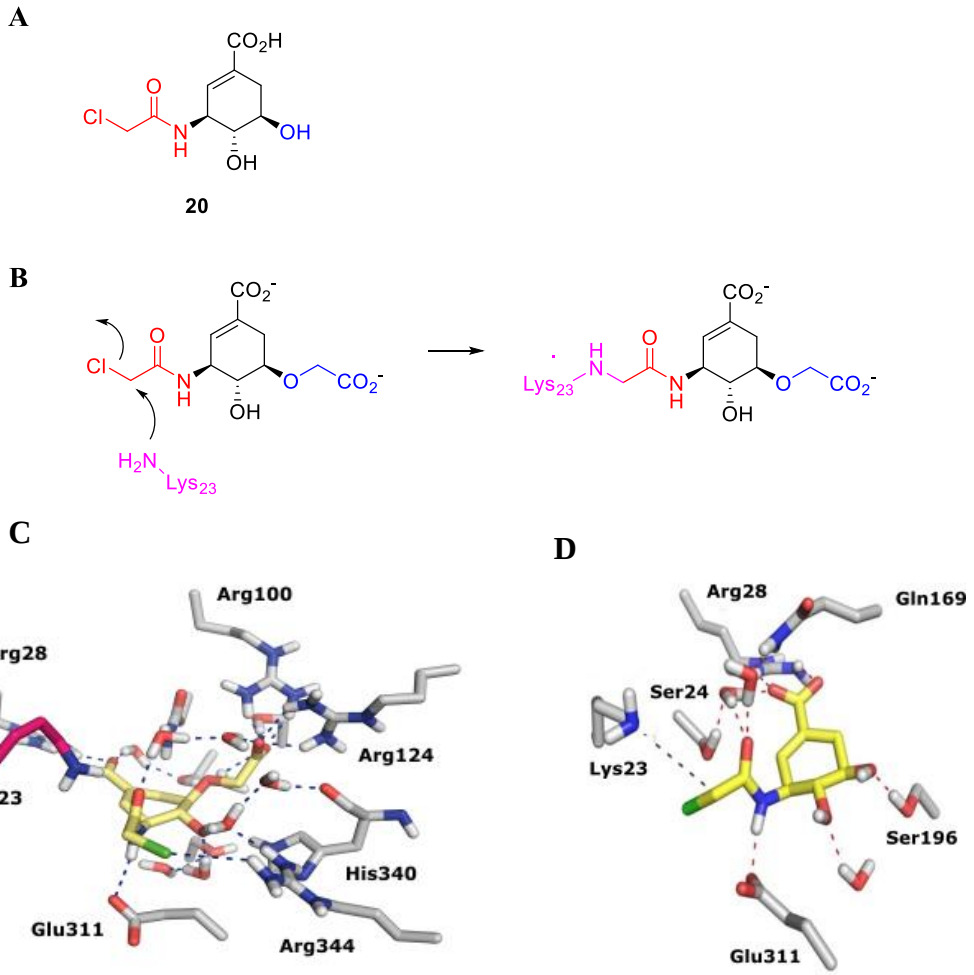

Figure 7*. (A) Amide* ***20*** *previously developed in the research group with excellent in vitro activity. (B) Proposed covalent modification mechanism of the EPSP synthase enzyme by target compound* ***19****. (C-D) Binding mode of compounds* ***19*** *(C) and* ***20*** *(D) in the EPSPS-Mt active site obtained by MD simulation studies. Relevant electrostatic and hydrogen bonding interactions are shown as blue dashed lines. Relevant side chain residues involved in ligand binding are shown and labeled. The residue Lys23 is highlighted in pink. Note the suitable arrangement of ε-amino group of residue Lys23 for reaction.*

Because of these positive results, we wanted to go one step further in this project by adding a carboxymethyl group in the C5 hydroxyl group in **20**. This group would mimic the substituent present in the natural substrate and would promote further strong interactions within the residues in the enzyme's active site (Figure 7C). In doing so, the covalent modification of EPSP synthase is predicted to be enhanced.

3 RESULTS AND DISCUSSION

The synthesis of the target amide **19** is proposed to be carried out from the amine **21**, whose preparation would be achieved in four steps from commercially available shikimic acid (**23**) (Scheme 5).

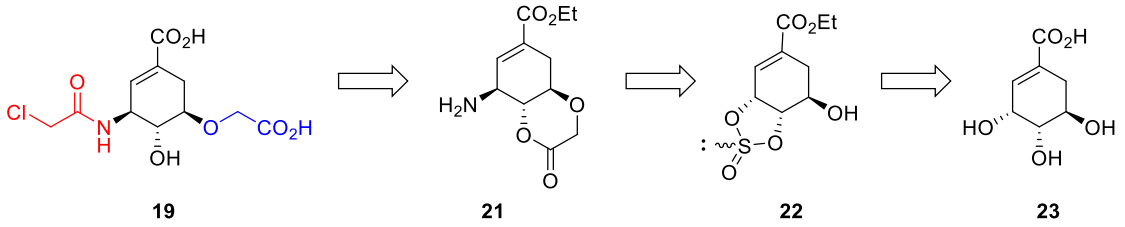

Scheme 5**. Retrosynthetic path of the target compound **19

Cyclic sulfite **22**[39] was prepared as previously described in two steps from (-)-shikimic acid (**23**) (Scheme 6). First, the esterification of (-)-shikimic acid (**23**) by heating in ethanol in an acidic medium afford ester **24**.[40] Second, treatment of triol **24** with thionyl chloride in the presence of dry triethylamine gave the cyclic sulfite **22** in 70% yield. The formation of **22** was confirmed by its spectroscopic data. Thus, the ^{1}H-NMR spectrum shows a characteristic quartet at 4.25 ppm with a J = 7 Hz that integrates by two hydrogen atoms, corresponding to the new CH_2 of the CO_2Et group. Also, the spectrum shows two multiplets, integrated each of them by one hydrogen atom, one at 5.57-5.54 ppm corresponding to H3, and another between 4.84 and 4.82 ppm corresponding to H4. The ^{13}C-NMR spectrum shows at 94.4 and 79.3 ppm the signals of both C3 and C4. It also shows at 167.2 ppm the signal corresponding to the CO_2Et group, whose presence is also confirmed by IR with a band centered at 1713 cm^{-1}. In addition, a broad band centered at 3487 cm^{-1} due to the free hydroxyl group is also observed. The data proved to be consistent with those previously described.

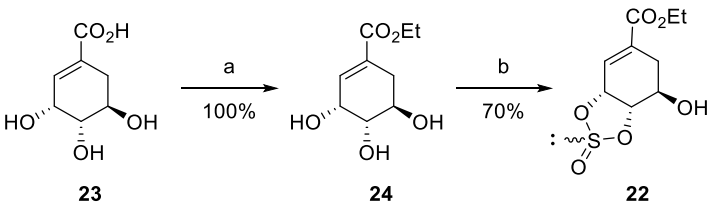

***Scheme 6**. Reagents and conditions: (a) EtOH, HCl(c), Δ. (b) $SOCl_2$, Et_3N, EtOAc, DCM, 0ºC to rt.*

The next step was the introduction of the 2-ethoxy-2-oxoethyl moiety in **22** by alkylation of its free hydroxyl group by treatment with ethyl diazoacetate and $Rh_2(OAc)_4$ as catalyst (Scheme 7). The ^{1}H-NMR spectrum of the resulting product, compound **25**, highlights

two multiplets, one between 4.28 and 4.18 ppm that integrates six hydrogen atoms, and the other between 1.34 and 1.25 ppm, integrating by six hydrogen atoms corresponding to the two methyl groups. The ^{13}C-NMR spectrum shows a signal at 170.1 ppm corresponding to the new carbonyl group in the scaffold. The IR spectrum reveals two characteristic bands centered at 1746 and 1713 cm^{-1}, corresponding to the two carbonyl groups. The structure of the compound was further corroborated by mass spectroscopy.

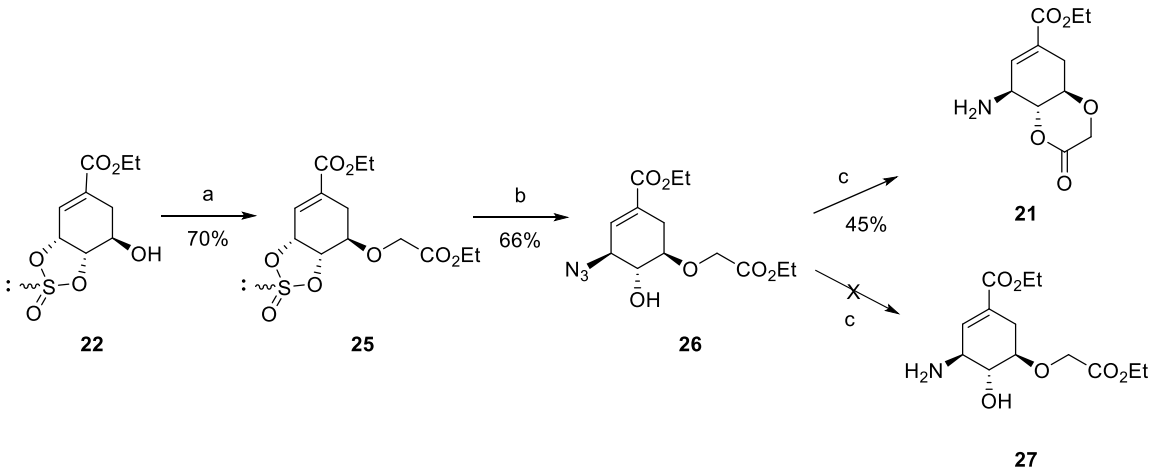

22 25 26 21 27

Scheme 7*. Reagents and conditions: (a) DAAE, $Rh_2(OAc)_4$, DCM, rt (b) NaN_3, DMF/H_2O (5:1), rt. (c) Ph_3P, THF, H_2O, Δ.*

The next step was the nucleophilic ring opening of the cyclic sulfite **25** by treatment with 2.5 equivalents of NaN_3[39] in aqueous DMF mixture at room temperature, obtaining compound **26** with a yield of 66%. The (R)-configuration of C3 was inverted into the (S)-configuration via a typical Walden-type inversion. In the ^{1}H-NMR spectrum highlights the displacement up-field of the signal of the H4 hydrogen atom that appeared at 5.05 ppm in the starting material and at 3.79 ppm in the product. Something similar happens with H3 hydrogen atom. The IR spectrum shows three bands centered at 3451, 2103, and 1713 cm^{-1}, corresponding to the hydroxyl group, azido, and the two carbonyl groups.

Next, the reduction of the azide **26** was carried out. Diverse methods were previously assayed in the research group, including reduction using sodium borohydride in the presence of $CoCl_2$[18], catalytic hydrogenation using Lindar[18] or Pd/C[41] catalyst. However, these methods showed to have distinct issues, such as simultaneous reduction of the double bond or cleavage of the ether bond. Among the three methods, hydrogenation using Lindar catalyst gave the desired product in 38% yield. Fortunately, the Staudinger reduction using triphenylphosphine gave good results.[18] It was observed that concomitant lactonization between the free hydroxyl group and the terminal ester group occurred. In

this project, this approach was optimized. Different conditions, solvents, and processing methods were tested. Initial attempts were carried out using methanol as solvent. However, as transesterification reactions were observed other solvents were assayed, specifically ethanol and THF. These modifications provided better results, but it was found difficult to isolate pure final product due to the formation of triphenylphosphine oxide. To overcome this issue, the use of triphenylphosphine supported on resin was attempted. Thus, treatment of azide **26** with 2.4 equivalents of Ph_3P resin in aqueous THF, and heating the mixture at 50 °C for days afforded the desired amine **21** with a yield of 45% and with >85% purity. Spectroscopic data shows an intramolecular cyclization reaction also occurred to give lactone **21**. The ^{1}H-NMR spectrum highlights two doublets appearing at 4.19 and 3.95 ppm with a J = 15.5 Hz, corresponding to the methylene group of the lactone. In addition, the spectrum shows two multiplets, one at 3.90-3.87 ppm integrated by two hydrogen atoms corresponding to H4 and H5, and another between 3.78 and 3.71 ppm integrated by one hydrogen atom corresponding to H3. The IR spectra reveals a band centered at 3097 cm^{-1} corresponding to the amine group and the absence of the band at 2103 cm^{-1} corresponding to the azido group in the starting material.

Next, for the introduction of the chloroacetyl chain at the C3 position several methods were tried. At first, the reaction was carried out by treatment of the amine **21** with chloroacetic acid, previously activated using EDC and DMAP.[18] After some time, once the reaction was worked out, the formation of amide **28** was not observed.

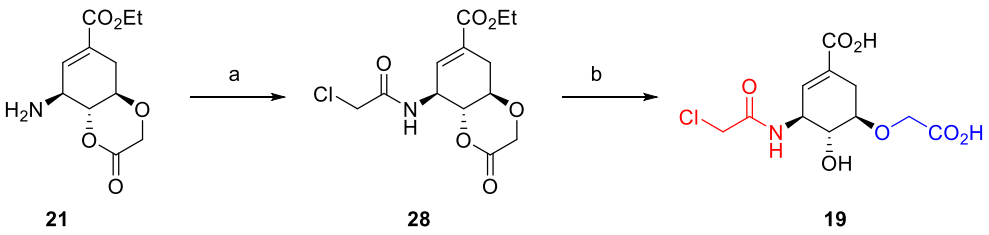

21 **28** **19**

Scheme 8. *Reagents and conditions: (a) $ClCH_2COCl$, Py, DCM, 0ºC to rt, (b) LiOH (aq), THF, rt.*

Alternatively, the formation of the amide bond was attempted using 2,5-dioxopyrrolidin-1-yl-2-chloroacetate (**30**), diisopropylethylamine and DMF as solvent. Mainly, we decided to try this reaction since *N*-hydroxysuccinimide esters are highly reactive. Compound **30** was synthesized following previously reported protocols from *N*-hydroxysuccinimide (**29**) and chloroacetyl chloride in chloroform and in the presence of

triethylamine, affording the desired compound with 90% yield (Scheme 9).[42] Unfortunately, peptide coupling also did not give good results.

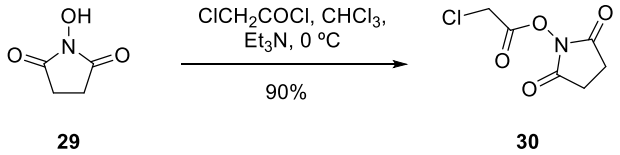

29 **30**

Scheme 9. *Synthesis of compound **30***

Fortunately, treatment of **21** with chloroacetyl chloride in the presence of Et_3N and dichloromethane as solvent gave the desired product **28** (Scheme 8). The ^{1}H-NMR spectrum shows the characteristic signal for a NH amide group at 6.97 ppm, as well as a singlet at 4.11 ppm, which integrates by two hydrogen atoms, corresponding to the methylene group of the chloroacetyl moiety. The mass spectra also confirmed the formation of amide **28** as the molecular ion (MH^+) was observed at 318. The presence of chlorine is further confirmed as the M^{+2} peak has an intensity of about one-third of the molecular ion peak (3:1 ratio). However, the reaction yield was 26%, which was relatively low since most of the product was lost during the processing step, and the compound was not completely purified after column chromatography. To enhance these results, Et_3N was changed to pyridine, keeping the rest of the conditions the same. As the elaboration process was more straightforward, since pyridine is easily eliminated by complexing with $CuSO_4$ (sat), the yield of the reaction was improved, reaching 90%. However, we were unable to get pure compound **28** and was used in the next step.

Finally, hydrolysis of ester **28** was performed by treatment with an aqueous solution of lithium hydroxide and subsequent protonation with the ion exchange resin Amberlite IR-120. In ^{1}H-NMR spectra of the resulting product, compound **19**, highlights the doublet at 4.28 ppm corresponding to the carboxymethoxy group, as well as the singlet at 4.14 ppm corresponding to the methylene group of the C3 chain. The mass spectra also corroborate the formation of the desired product since the molecular ion (MH^+) was observed at 308.05, which coincides with the expected mass for **19**. The final product was not fully characterized due to the lack of time and sample.

4 EXPERIMENTAL PROCEDURE

4.1 Methods and Equipment

The reactions were monitored by thin-layer chromatography using 20 × 20 cm aluminum plates with silica gel 60 F_{254} (Merck). The spots were visualized with UV light (254 nm) and exposed with Ce/Mo solutions (Hanessian), ninhydrin, and in some cases, permanganate. Purification of the compounds was performed by flash chromatography using silica gel 60 (230-400 mesh, ASTM, VWR) as a stationary phase.

NMR spectra were recorded on a VARIAN Mercury-300 spectrometer in deuterated solvents. All assignments were performed by ^{1}H-NMR, ^{13}C-NMR with broadband decoupling, and DEPT-135. Chemical shifts (δ) are given in ppm and coupling constants (J) in hertz.

IR spectra were recorded on a PerkinElmer Two FTIR spectrometer with attenuated total reference (ATR).

Mass spectra were recorded on a Bruker Microtof ESI-TOF spectrometer using electrospray ionization (ESI) as the ionization procedure. The data obtained is expressed in mass units (m/z).

Optical rotations were determined using a Jasco DIP-370 automatic polarimeter and are expressed in 10^{-1} degrees cm^2 g^{-1}.

Water was used, deionized, and purified in a Millipore Milli-Q-POD.

The graphical representations of the proteins and their ligands were made using the PyMOL program.[43]

4.2 Preparation of compound 22

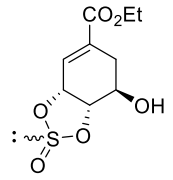

22

A solution of commercially available (-)-shikimic acid (**23**) (10 g, 57.4 mmol) in ethanol (82 mL) and HCl (c) (3.4 mL) was heated at reflux for 20 h. After cooling to room temperature, the reaction mixture was concentrated under reduced pressure and the crude mixture (16.4 g, 81.3 mmol) was dissolved in ethyl acetate (325 mL) under an inert atmosphere, cooled to 0 °C and then treated with dry triethylamine (17.3 mL, 203.25 mmol). A solution of thionyl chloride (14.8 mL, 203.25 mmol) in dry dichloromethane (50.8 mL) was added dropwise and the reaction mixture was stirred at room temperature for 22 h. The reaction was quenched by adding water (~ 20 mL) and an aqueous solution of potassium carbonate until reaching a pH around 8-9. The organic layer was separated, and the aqueous phase was extracted with diethyl ether (x3). The organic extracts were combined, dried (anh. Na_2SO_4), filtered, and concentrated under reduced pressure. The resulting residue was purified by flash chromatography on silica gel, using (5:95) MeOH/CH_2Cl_2 as eluent, to get the sulfite **22** (5.61 g, 56%) as a yellow oil. ^{1}H-NMR (300 MHz, $CDCl_3$) δ: 6.92 (m, 1H, H2), 5.57-5.54 (m, 1H, H3), 4.84-4.82 (m, 1H, H4), 4.25 (q, *J* = 7.1 Hz, 2H, CH_2), 3.96-3.93 (m, 1H, H5), 2.88 (dd, *J* = 4.9 and 18.1 Hz, 1H, C*H*H-6), 2.33 (dd, *J* = 8.5 and 17.9 Hz, 1H, CH*H*-6), 1.32 (t, *J* = 7.1 Hz, 3H, CH_3) ppm. ^{13}C-NMR (63 MHz, $CDCl_3$) δ: 167.2 (C), 137.7 (CH), 128.3 (C), 94.4 (CH), 79.3 (CH), 63.5 (CH), 61.7 (CH_2), 31.7 (CH_2), 14.2 (CH_3) ppm. IR (ATR): 3487 (OH) and 1718 (CO) cm^{-1}. The spectroscopic data was in agreement with previously reported results by Liang-Deng Nie *et al*.

4.3 Preparation of compound 25

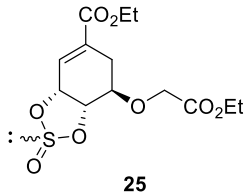

25

A solution of the sulfite **22** (1.19 g, 4.81 mmol) and $Rh_2(OAc)_4$ (34 mg, 77 μmol) in dry dichloromethane (3.2 mL) was treated dropwise for about 1 h with a previously prepared solution of ethyl diazoacetate (1 mL, 9.63 mmol) in dry dichloromethane (9.6 mL, 1 M). The reaction mixture was stirred at room temperature for 1 h during which time the solution becomes medium brown. The solvent was concentrated under reduced pressure and the crude was purified by flash chromatography on silica gel using (40:60) ethyl acetate/hexane as eluent. The ether **25** (0.84 g, 70%) was obtained as a yellow oil. $[\alpha]_D^{20}$ = +83.5° (c 1.0, $CHCl_3$). ^{1}H-NMR (300 MHz, $CDCl_3$) δ: 6.88 (m, 1H, H2), 5.59-5.56 (m, 1H, H3), 5.05 (t, *J* = 6.7 Hz, 1H, H4), 4.28-4.18 (m, 6H, 3×CH_2), 3.86-3.79 (m, 1H, H5), 2.88 (dd, *J* = 4.7 and 18.2 Hz, 1H, C*H*H-6), 2.46 (dd, *J* = 7.3 and 18.2 Hz, 1H, CH*H*-6), 1.34-1.25 (m, 6H, 2×CH_3) ppm. ^{13}C-NMR (63 MHz, $CDCl_3$) δ: 170.1 (C), 165.4 (C), 132.7 (C), 129.4 (CH), 79.3 (CH), 76.3 (CH), 75.5 (CH), 67.9 (CH_2), 61.7 (CH_2), 61.3 (CH_2), 27.3 (CH_2), 14.3 (CH_3), 14.3 (CH_3) ppm. IR (ATR): 1746 (CO) and 1713 (CO) cm^{-1}. MS (ESI) m/z = 357 (MNa^+). HRMS calculated for $C_{13}H_{18}O_8SNa$ (MNa^+): 357.0615; found, 357.0616.

4.4 Preparation of compound 26

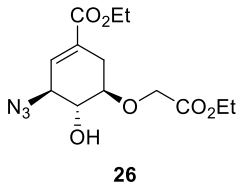

26

A solution of the cyclic sulfite **25** (835.5 mg, 2.50 mmol) in DMF (10.4 mL) and water (2.1 mL) at room temperature was treated with sodium azide (410 mg, 6.25 mmol) and stirred for 24 h. During this time a change of color from strong yellow to pale yellow was observed. The reaction mixture was diluted with ethyl acetate and water in a 1:4 ratio. The organic phase was separated, and the aqueous layer was extracted with ethyl acetate

(x2). The organic phases were combined and successively washed with water and brine. The organic extract was dried (anh. Na_2SO_4), filtered, and concentrated under reduced pressure. The crude mixture was purified by flash chromatography on silica gel, eluting with (70:30) ethyl acetate/hexane, to obtain the azide **26** (438.8 mg, 66%) as a yellow oil. $[\alpha]_D^{20} = -6.8°$ (c 1.0, $CHCl_3$). ^{1}H-NMR (300 MHz, $CDCl_3$) δ: 6.61 (m, 1H, H2), 4.40-4.13 (m, 7H, 3xCH_2, H3), 3.79 (t, *J* = 9 Hz, 1H, H4), 3.53-3.44 (td, *J* = 5.7 and 9.9 Hz, 1H, H5), 2.95 (dd, *J* = 6 and 18 Hz, 1H, C*H*H-6), 2.30-2.04 (m, 1H, CH*H*-6), 1.30 (t, *J* = 6 Hz, 6H, 2xCH_3) ppm. ^{13}C-NMR (63 MHz, $CDCl_3$) δ: 171.6 (CO), 165.4 (CO), 134.3 (C), 129.8 (C), 80.0 (CH), 74.3 (CH), 67.3 (CH_2), 63.8 (CH), 61.6 (CH_2), 61.2 (CH_2), 29.7 (CH_2), 14.2 (CH_3), 14.1 (CH_3) ppm. IR (ATR): 3451 (OH), 2103 (N_3) and 1713 (CO) cm^{-1}. MS (ESI) m/z = 336 (MNa^+). HRMS calculated for $C_{13}H_{19}N_3NaO_6$ (MNa^+): 336.1166; found, 336.1172.

4.5 Preparation of compound 21

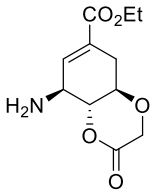

21

A solution of the azide **26** (200 mg, 0.64 mmol) in a (1:1) mixture of THF/H_2O (21.4 mL) at room temperature was treated with triphenylphosphine resin (402.9 mg, 1.54 mmol) and then heated at 50 °C for four days. After cooling to room temperature, the suspension was filtered and washed with THF. The filtrate and the washings were concentrated and the remaining water was eliminated by lyophilization. The amine **21** (90 mg, 45%) was obtained as a pale-yellow oil. $[\alpha]_D^{20}$ = -39.5° (*c* 1.0, MeOH). ^{1}H-NMR (300 MHz, CD_3OD) δ: 6.76 (m, 1H, H2), 4.29 (q, *J* = 7.1 Hz, 2H, C*H*$_2$$CH_3$), 4.19 (d, *J* = 15.5 Hz, 1H, COOC*H*H), 3.95 (d, *J* =15.5 Hz, 1H, COOCH*H*), 3.90-3.87 (m, 2H, H4+H5), 3.78-3.71 (m, 1H, H3), 2.91 (dd, *J* = 5.4 and 18.4 Hz, 1H, C*H*H-6), 2.44 (dd, *J* = 7.0 and 18.1 Hz, 1H, CH*H*-6), 1.36 (t, *J* = 7.2 Hz, 3H, CH_3) ppm. ^{13}C-NMR (63 MHz, CD_3OD) δ: 176.8 (C), 165.5 (C), 132.5 (C), 130.2 (CH), 77.4 (CH), 69.4 (CH), 69.2 (CH_2), 60.9 (CH_2), 52.6 (CH), 28.3 (CH_2), 13.0 (CH_3) ppm. IR (ATR): 3097 (NH), 1719 (CO) and 1578 (CO) cm^{-1}. MS (ESI) m/z = 242.1 (MH^+).

4.6 Preparation of compound 28

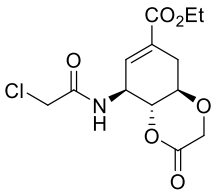

28

Method A

A solution of the amine **21** (75.4 mg, 0.31 mmol) in dry dichloromethane (3.1 mL), under an inert atmosphere at 0 ºC, was successively treated with dry pyridine (30 μL, 0.38 mmol) and a previously prepared solution of chloride chloroacetate (27 μL, 0.34 mmol) in dry dichloromethane (0.3 mL). It was stirred for 15 min at 0 ºC and 3 h at room temperature. The reaction mixture was diluted with dichloromethane and water, the aqueous phase was separated, and the organic layer was washed successively with saturated solution of $CuSO_4$ (x3). The organic extract was dried (anh. Na_2SO_4), filtered, and concentrated under reduced pressure, to afford the crude amide **28**.

Method B

A solution of the amine **21** (80 mg, 0.33 mmol) in dry dichloromethane (3.3 mL), under an inert atmosphere at 0 ºC, was successively treated with dry Et_3N (56 μL, 0.40 mmol) and a previously prepared solution of chloride chloroacetate (29 μL, 0.37 mmol) in dry dichloromethane (0.4 mL). It was stirred for 15 min at 0 ºC and 3 h at room temperature. The reaction mixture was diluted with dichloromethane (3 mL) and HCl (10%) (3 mL). The aqueous phase was separated, and the organic layer was washed successively with saturated $NaHCO_3$ and brine. The organic extract was dried (anh Na_2SO_4), filtered, and concentrated under reduced pressure, to afford the crude amide **28**.

4.7 Preparation of compound 19

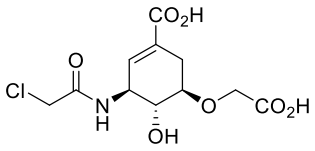

19

A solution of the crude amide **28** (86 mg, 0.27 mmol) in THF (2.7 mL) was treated with an aqueous lithium hydroxide solution (2.7 mL, 0.5 M) and the reaction mixture was stirred at room temperature for 2 h. Milli-Q water was added, and the THF was concentrated under reduced pressure. The aqueous residue obtained was washed with diethyl ether (×3), and the aqueous phase was treated with Amberlite IR-120 (H^+), up to pH 6. The resin was filtered and washed with Milli-Q water. The filtrate and washings were lyophilized, providing the crude (48.1 mg) as a white solid, which was purified by reverse phase obtaining the compound **19** (15 mg, 31%). ^{1}H-NMR (300 MHz, D_2O) δ: 6.55 (m, 1H, H2), 4.60-4.54 (m, 1H, H3), 4.28 (d, *J* = 8.0 Hz, 2H, OCH_2), 4.14 (s, 2H, $COCH_2Cl$), 3.84-3.73 (m, 2H, H4+H5), 2.90 (dd, *J* = 4.9 and 17.1 Hz, 1H, C*H*H-6), 2.27 (dd, *J* = 8.1 and 14.3 Hz, 1H, CH*H*-6) ppm. IR (ATR): 3431 (NH+OH), 1719 (CO) and 1653 (CO) cm^{-1}. MS (ESI) m/z = 308.0 (MH^+). HRMS calculated for $C_{11}H_{15}ClNO_7$ (MH^+): 308.0532; found, 308.0529.

5 CONCLUSIONS

From the results obtained, we can conclude that:

- The synthesis of target compound **19** was carried out in seven steps from commercially available (-)-shikimic acid (**23**).
- The key step is the nucleophilic ring opening of cyclic sulfite (**25**) by sodium azide.
- The reduction of the azide intermediate **26** undergoes with concomitant intramolecular lactonization between the secondary hydroxyl group and the terminal carboxylate group.

De los resultados obtenidos se puede concluir que:

- La síntesis del compuesto diana **19** se llevó a cabo en siete pasos a partir del ácido (-)-siquímico (**23**) comercial.
- El paso clave es la apertura nucleofílica del anillo del sulfito cíclico (**25**) con azida sódica.
- La reducción del intermedio azida **26** se produce con la lactonización intramolecular entre el grupo hidroxilo secundario y el grupo carboxilato terminal.

Dos resultados obtidos pódese concluir que:

- A síntese do composto diana **19** levouse a cabo en sete pasos a partir do ácido (-)-siquímico (**23**) comercial.
- O paso clave é a apertura nucleofílica do anel do sulfito cíclico (**25**) con azida sódica.
- A redución do intermedio azida **26** prodúcese coa lactonización intramolecular entre o grupo hidroxilo secundario e o grupo carboxilato terminal.

6 REFERENCES

(1) *It's time to fix the antibiotic market*. Wellcome. https://wellcome.org/news/its-time-fix-antibiotic-market (accessed Jun 17, 2022).

(2) Sánchez-López, E.; Gomes, D.; Esteruelas, G.; Bonilla, L.; Lopez-Machado, A. L.; Galindo, R.; Cano, A.; Espina, M.; Ettcheto, M.; Camins, A.; Silva, A. M.; Durazzo, A.; Santini, A.; Garcia, M. L.; Souto, E. B. Metal-Based Nanoparticles as Antimicrobial Agents: An Overview. *Nanomaterials.* **2020**, *10* (2), 292. https://doi.org/10.3390/nano10020292.

(3) Reygaert, W. C. An Overview of the Antimicrobial Resistance Mechanisms of Bacteria. *AIMS Microbiol.* **2018**, *4* (3), 482–501. https://doi.org/10.3934/microbiol.2018.3.482.

(4) Cooper, M. A.; Shlaes, D. Fix the Antibiotics Pipeline. *Nature.* **2011**, *472* (7341), 32–32. https://doi.org/10.1038/472032a.

(5) García, F. Resistencia bacteriana a antibióticos. *Acta Médica Costarric.* **2001**, *43* (3), 101–102.

(6) Von Döhren, H. Antibiotics: Actions, Origins, Resistance. *Protein Sci. Publ. Protein Soc.* **2004**, *13* (11), 3059–3060. https://doi.org/10.1110/ps.041032204.

(7) Aminov, R. History of Antimicrobial Drug Discovery: Major Classes and Health Impact. *Biochem. Pharmacol.* **2017**, *133*, 4–19. https://doi.org/10.1016/j.bcp.2016.10.001.

(8) González-Bello, C. Antibiotic Adjuvants – A Strategy to Unlock Bacterial Resistance to Antibiotics. *Bioorg. Med. Chem. Lett.* **2017**, *27* (18), 4221–4228. https://doi.org/10.1016/j.bmcl.2017.08.027.

(9) Murray, C. J.; Ikuta, K. S.; Sharara, F.; Swetschinski, L.; Robles Aguilar, G.; Gray, A.; Han, C.; Bisignano, C.; Rao, P.; Wool, E.; Johnson, S. C.; Browne, A. J.; Chipeta, M. G.; Fell, F.; Hackett, S.; Haines-Woodhouse, G.; Kashef Hamadani, B. H.; Kumaran, E. A. P.; McManigal, B.; Agarwal, R.; Akech, S.; Albertson, S.; Amuasi, J.; Andrews, J.; Aravkin, A.; Ashley, E.; Bailey, F.; Baker, S.; Basnyat, B.; Bekker, A.; Bender, R.; Bethou, A.; Bielicki, J.; Boonkasidecha, S.; Bukosia, J.; Carvalheiro, C.; Castañeda-Orjuela, C.; Chansamouth, V.; Chaurasia, S.; Chiurchiù, S.; Chowdhury, F.; Cook, A. J.; Cooper, B.; Cressey, T. R.; Criollo-Mora, E.; Cunningham, M.; Darboe, S.; Day, N. P. J.; De Luca, M.; Dokova, K.; Dramowski, A.; Dunachie, S. J.; Eckmanns, T.; Eibach, D.; Emami, A.; Feasey, N.; Fisher-Pearson, N.; Forrest, K.; Garrett, D.; Gastmeier, P.; Giref, A. Z.; Greer, R. C.; Gupta, V.; Haller, S.; Haselbeck, A.; Hay, S. I.; Holm, M.; Hopkins, S.; Iregbu, K. C.; Jacobs, J.; Jarovsky, D.; Javanmardi, F.; Khorana, M.; Kissoon, N.; Kobeissi, E.; Kostyanev, T.; Krapp, F.; Krumkamp, R.; Kumar, A.; Kyu, H. H.; Lim, C.; Limmathurotsakul, D.; Loftus, M. J.; Lunn, M.; Ma, J.; Mturi, N.; Munera-Huertas, T.; Musicha, P.; Mussi-Pinhata, M. M.; Nakamura, T.; Nanavati, R.; Nangia, S.; Newton, P.;

Ngoun, C.; Novotney, A.; Nwakanma, D.; Obiero, C. W.; Olivas-Martinez, A.; Olliaro, P.; Ooko, E.; Ortiz-Brizuela, E.; Peleg, A. Y.; Perrone, C.; Plakkal, N.; Ponce-de-Leon, A.; Raad, M.; Ramdin, T.; Riddell, A.; Roberts, T.; Robotham, J. V.; Roca, A.; Rudd, K. E.; Russell, N.; Schnall, J.; Scott, J. A. G.; Shivamallappa, M.; Sifuentes-Osornio, J.; Steenkeste, N.; Stewardson, A. J.; Stoeva, T.; Tasak, N.; Thaiprakong, A.; Thwaites, G.; Turner, C.; Turner, P.; van Doorn, H. R.; Velaphi, S.; Vongpradith, A.; Vu, H.; Walsh, T.; Waner, S.; Wangrangsimakul, T.; Wozniak, T.; Zheng, P.; Sartorius, B.; Lopez, A. D.; Stergachis, A.; Moore, C.; Dolecek, C.; Naghavi, M. Global Burden of Bacterial Antimicrobial Resistance in 2019: A Systematic Analysis. *The Lancet.* **2022**, *399* (10325), 629–655. https://doi.org/10.1016/S0140-6736(21)02724-0.

(10) Papp-Wallace, K. M.; Endimiani, A.; Taracila, M. A.; Bonomo, R. A. Carbapenems: Past, Present, and Future. *Antimicrob. Agents Chemother.* **2011**, *55* (11), 4943–4960. https://doi.org/10.1128/AAC.00296-11.

(11) Spagnolo, A. M.; Sartini, M.; Cristina, M. L. Pseudomonas Aeruginosa in the Healthcare Facility Setting. *Rev. Res. Med. Microbiol.* **2021**, *32* (3), 169–175. https://doi.org/10.1097/MRM.0000000000000271.

(12) Thomsen, T. T.; Biology, M. Peptide Antibiotics for ESKAPE Pathogens. Ph.D. Thesis, University of Copenhagen, Denmark, January 2016.

(13) Kohanski, M. A.; Dwyer, D. J.; Collins, J. J. How Antibiotics Kill Bacteria: From Targets to Networks. *Nat. Rev. Microbiol.* **2010**, *8* (6), 423–435. https://doi.org/10.1038/nrmicro2333.

(14) Aslam, B.; Wang, W.; Arshad, M. I.; Khurshid, M.; Muzammil, S.; Rasool, M. H.; Nisar, M. A.; Alvi, R. F.; Aslam, M. A.; Qamar, M. U.; Salamat, M. K. F.; Baloch, Z. Antibiotic Resistance: A Rundown of a Global Crisis. *Infect. Drug Resist.* **2018**, *Volume 11*, 1645–1658. https://doi.org/10.2147/IDR.S173867.

(15) Burmeister, A. R. Horizontal Gene Transfer. *Evol. Med. Public Health.* **2015**, *2015* (1), 193–194. https://doi.org/10.1093/emph/eov018.

(16) Chellat, M. F.; Raguž, L.; Riedl, R. Targeting Antibiotic Resistance. *Angew. Chem. Int. Ed.* **2016**, *55* (23), 6600–6626. https://doi.org/10.1002/anie.201506818.

(17) Prado, V.; Lence, E.; Maneiro, M.; Vázquez-Ucha, J. C.; Beceiro, A.; Thompson, P.; Hawkins, A. R.; González-Bello, C. Targeting the Motion of Shikimate Kinase: Development of Competitive Inhibitors That Stabilize an Inactive Open Conformation of the Enzyme. *J. Med. Chem.* **2016**, *59* (11), 5471–5487. https://doi.org/10.1021/acs.jmedchem.6b00483.

(18) López, V. P. Inhibidores de la siquimato quinasa para el tratamiento de infecciones bacterianas: diseño, síntesis y evaluación biológica. Ph.D. Thesis [Online]. Universidade

de Santiago de Compostela, 2016. http://purl.org/dc/dcmitype/Text (accessed Jun 10, 2022).

(19) Herrmann, K. M.; Weaver, L. M. The Shikimate Pathway. **1999**, 32.

(20) Blanco, B.; Prado, V.; Lence, E.; Otero, J. M.; Garcia-Doval, C.; van Raaij, M. J.; Llamas-Saiz, A. L.; Lamb, H.; Hawkins, A. R.; González-Bello, C. Mycobacterium Tuberculosis Shikimate Kinase Inhibitors: Design and Simulation Studies of the Catalytic Turnover. *J. Am. Chem. Soc.* **2013**, *135* (33), 12366–12376. https://doi.org/10.1021/ja405853p.

(21) Krishnan, A.; Kloehn, J.; Lunghi, M.; Soldati-Favre, D. Vitamin and Cofactor Acquisition in Apicomplexans: Synthesis versus Salvage. *J. Biol. Chem.* **2020**, *295* (3), 701–714. https://doi.org/10.1074/jbc.AW119.008150.

(22) Ribeiro Marques, M.; Henrique Pereira, J.; Oliveira, J.; Augusto Basso, L.; Filgueira de Azevedo, W.; Santiago Santos, D.; Sergio Palma, M. The Inhibition of 5-Enolpyruvylshikimate-3-Phosphate Synthase as a Model for Development of Novel Antimicrobials. *Curr. Drug Targets.* **2007**, *8* (3), 445–457. https://doi.org/10.2174/138945007780058951.

(23) *DEG*. http://origin.tubic.org/deg/public/index.php (accessed Jun 17, 2022).

(24) Umland, T. C.; Schultz, L. W.; MacDonald, U.; Beanan, J. M.; Olson, R.; Russo, T. A. *In Vivo* -Validated Essential Genes Identified in Acinetobacter Baumannii by Using Human Ascites Overlap Poorly with Essential Genes Detected on Laboratory Media. *mBio*. **2012**, *3* (4), e00113-12. https://doi.org/10.1128/mBio.00113-12.

(25) Stritzker, J.; Janda, J.; Schoen, C.; Taupp, M.; Pilgrim, S.; Gentschev, I.; Schreier, P.; Geginat, G.; Goebel, W. Growth, Virulence, and Immunogenicity of *Listeria Monocytogenes Aro* Mutants. *Infect. Immun.* **2004**, *72* (10), 5622–5629. https://doi.org/10.1128/IAI.72.10.5622-5629.2004.

(26) Schönbrunn, E.; Eschenburg, S.; Shuttleworth, W. A.; Schloss, J. V.; Amrhein, N.; Evans, J. N. S.; Kabsch, W. Interaction of the Herbicide Glyphosate with Its Target Enzyme 5-Enolpyruvylshikimate 3-Phosphate Synthase in Atomic Detail. *Proc. Natl. Acad. Sci.* **2001**, *98* (4), 1376–1380. https://doi.org/10.1073/pnas.98.4.1376.

(27) Bank, R. P. D. *RCSB PDB - 2BJB: Mycobacterium Tuberculosis Epsp Synthase In Unliganded State*. https://www.rcsb.org/structure/2BJB (accessed Jun 20, 2022).

(28) Bank, R. P. D. *RCSB PDB - 2O0E: Mycobacterium tuberculosis epsp synthase in complex with S3P and PEP*. https://www.rcsb.org/structure/2O0E (accessed Jun 20, 2022).

(29) Anderson, K. S.; Sikorski, J. A.; Johnson, K. A. A Tetrahedral Intermediate in the EPSP Synthase Reaction Observed by Rapid Quench Kinetics. *Biochemistry.* **1988**, *27* (19), 7395–7406. https://doi.org/10.1021/bi00419a034.

(30) Gawuga, V. Design and Synthesis of Potential Inhibitors of Enolpyruvyl Shikimate 3-Phosphate Synthase (EPSPS). Thesis, McMaster University, Ontario, September 2008.

(31) Funke, T.; Han, H.; Healy-Fried, M. L.; Fischer, M.; Schönbrunn, E. Molecular Basis for the Herbicide Resistance of Roundup Ready Crops. *Proc. Natl. Acad. Sci.* **2006**, *103* (35), 13010–13015. https://doi.org/10.1073/pnas.0603638103.

(32) Alberg, D. G.; Bartlett, P. A. Potent Inhibition of 5-Enolpyruvylshikimate-3-Phosphate Synthase by a Reaction Intermediate Analog. *J. Am. Chem. Soc.* **1989**, *111* (6), 2337–2338. https://doi.org/10.1021/ja00188a078.

(33) Miller, M. J.; Cleary, D. G.; Ream, J. E.; Snyder, K. R.; Sikorski, J. A. New EPSP Synthase Inhibitors: Synthesis and Evaluation of an Aromatic Tetrahedral Intermediate Mimic Containing a 3-Malonate Ether as a 3-Phosphate Surrogate. *Bioorg. Med. Chem.* **1995**, *3* (12), 1685–1692. https://doi.org/10.1016/0968-0896(95)00156-5.

(34) Peterson, M. L.; Corey, S. D.; Font, J. L.; Walker, M. C.; Sikorski, J. A. New Simplified Inhibitors of EPSP Synthase: The Importance of Ring Size for Recognition at the Shikimate 3-Phosphate Site. *Bioorg. Med. Chem. Lett.* **1996**, *6* (23), 2853–2858. https://doi.org/10.1016/S0960-894X(96)00527-6.

(35) Bauer, R. A. Covalent Inhibitors in Drug Discovery: From Accidental Discoveries to Avoided Liabilities and Designed Therapies. *Drug Discov. Today.* **2015**, *20* (9), 1061–1073. https://doi.org/10.1016/j.drudis.2015.05.005.

(36) González-Bello, C. Designing Irreversible Inhibitors--Worth the Effort? *ChemMedChem.* **2016**, *11* (1), 22–30. https://doi.org/10.1002/cmdc.201500469.

(37) Maneiro, M.; Lence, E.; Sanz-Gaitero, M.; Otero, J. M.; van Raaij, M. J.; Thompson, P.; Hawkins, A. R.; González-Bello, C. Hydroxylammonium Derivatives for Selective Active-Site Lysine Modification in the Anti-Virulence Bacterial Target DHQ1 Enzyme. *Org. Chem. Front.* **2019**, *6* (17), 3127–3135. https://doi.org/10.1039/C9QO00453J.

(38) Søndergaard, C. R.; Olsson, M. H. M.; Rostkowski, M.; Jensen, J. H. Improved Treatment of Ligands and Coupling Effects in Empirical Calculation and Rationalization of pK_a Values. *J. Chem. Theory Comput.* **2011**, *7* (7), 2284–2295. https://doi.org/10.1021/ct200133y.

(39) Nie, L.-D.; Shi, X.-X.; Quan, N.; Wang, F.-F.; Lu, X. Novel Asymmetric Synthesis of Oseltamivir Phosphate (Tamiflu) from (−)-Shikimic Acid via Cyclic Sulfite Intermediates. *Tetrahedron Asymmetry.* **2011**, *22* (16–17), 1692–1699. https://doi.org/10.1016/j.tetasy.2011.09.014.

(40) Federspiel, M.; Fischer, R.; Hennig, M.; Mair, H-J.; Oberhauser, T.; Rimmler, G.; Albiez, T.; Bruhin, J.; Estermann, H.; Gandert, C.; Gockel, V.; Gotzo, S.; Hoffmann, U.; Huber, G.; Janatsch, G.; Lauper, S.; Rockel-Stabler, O.; Trussardi, R.; Zwahlen, AG. *Org Process Res 45 Dev.* **1999**, *3*, 266−274.

(41) Valverde, L. T. La Inhibición de los enzimas deshidroquinasa Tipo I y II: una estrategia para el desarrollo de nuevos antibióticos. Ph.D. Thesis [Online], Universidade de Santiago de Compostela, 2012. http://purl.org/dc/dcmitype/Text (accessed Jun 10, 2022).

(42) Gray, N.; Lim, S.; Choi, H.; Westover, K. Ras Inhibitors and Uses Thereof. PCT/US2014/026033, October 2, 2014.

(43) *PyMOL | pymol.org*. https://pymol.org/2/ (accessed May 20, 2022).

APPENDIX. SPECTRA

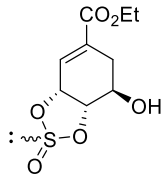

22

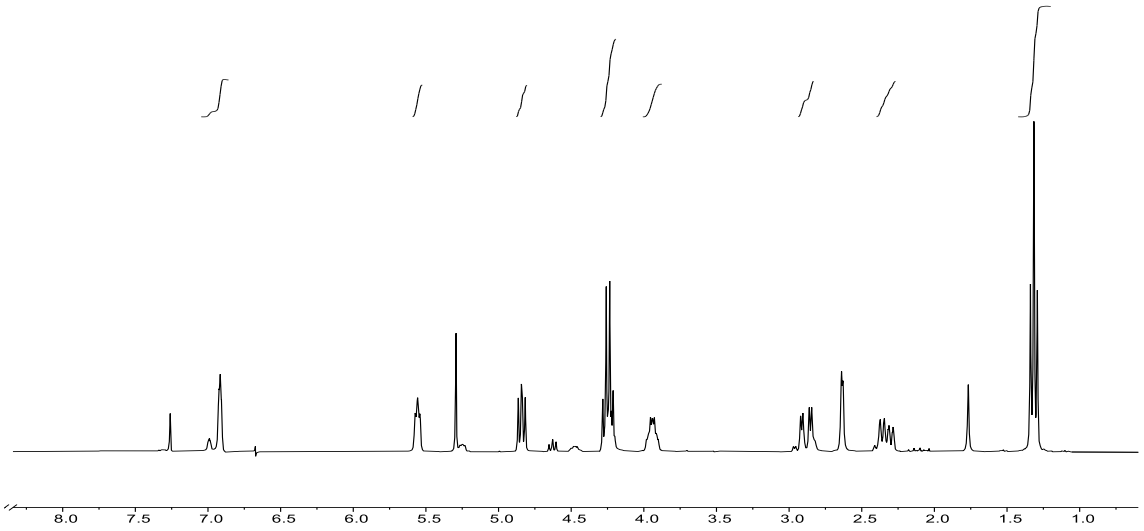

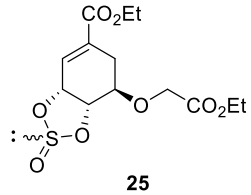

25

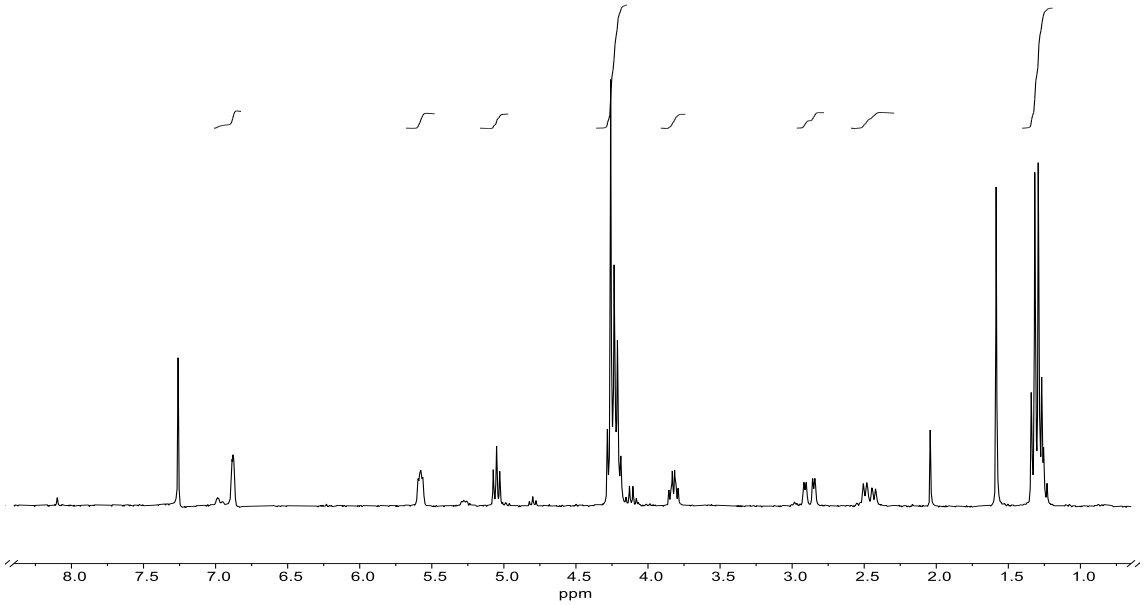

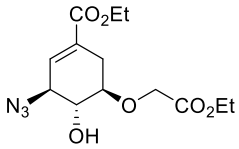
CO2Et
N3
O
CO2Et
OH

26

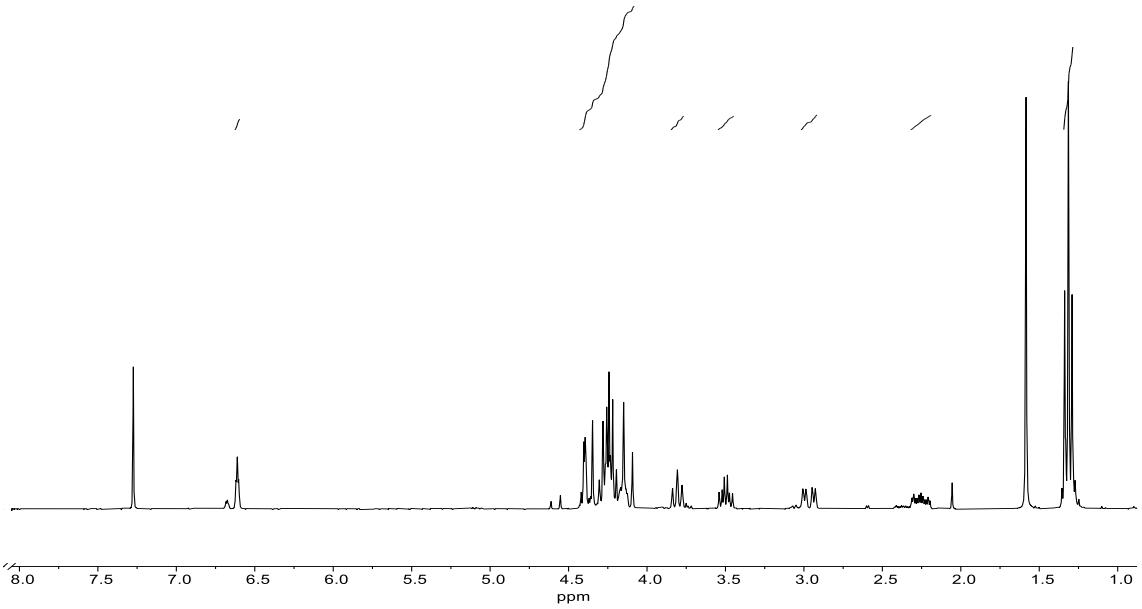
8.0
7.5
7.0
6.5
6.0
5.5
5.0
4.5
4.0
3.5
3.0
2.5
2.0
1.5
1.0
ppm

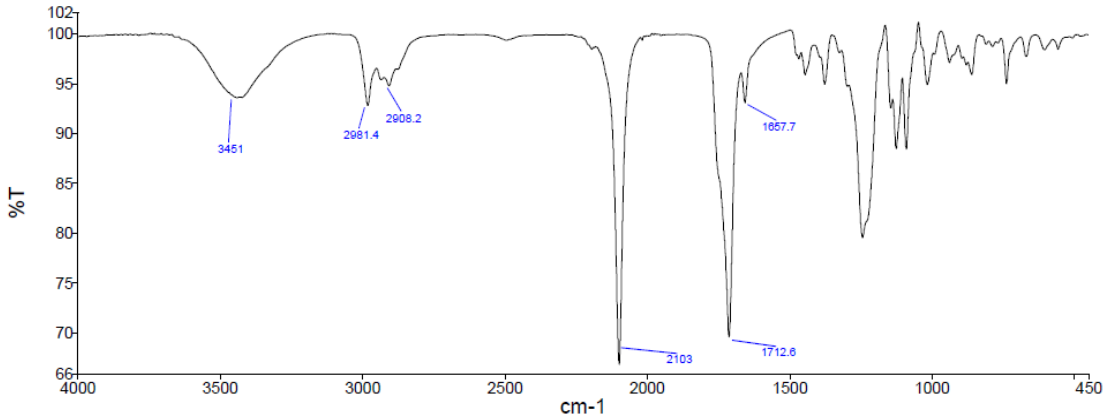
%T
102
100
95
90
85
80
75
70
66
3451
2981.4
2908.2
2103
1712.6
1657.7
4000
3500
3000
2500
2000
1500
1000
450
cm-1

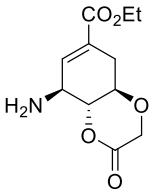
CO2Et
H2N
O
O
O

21

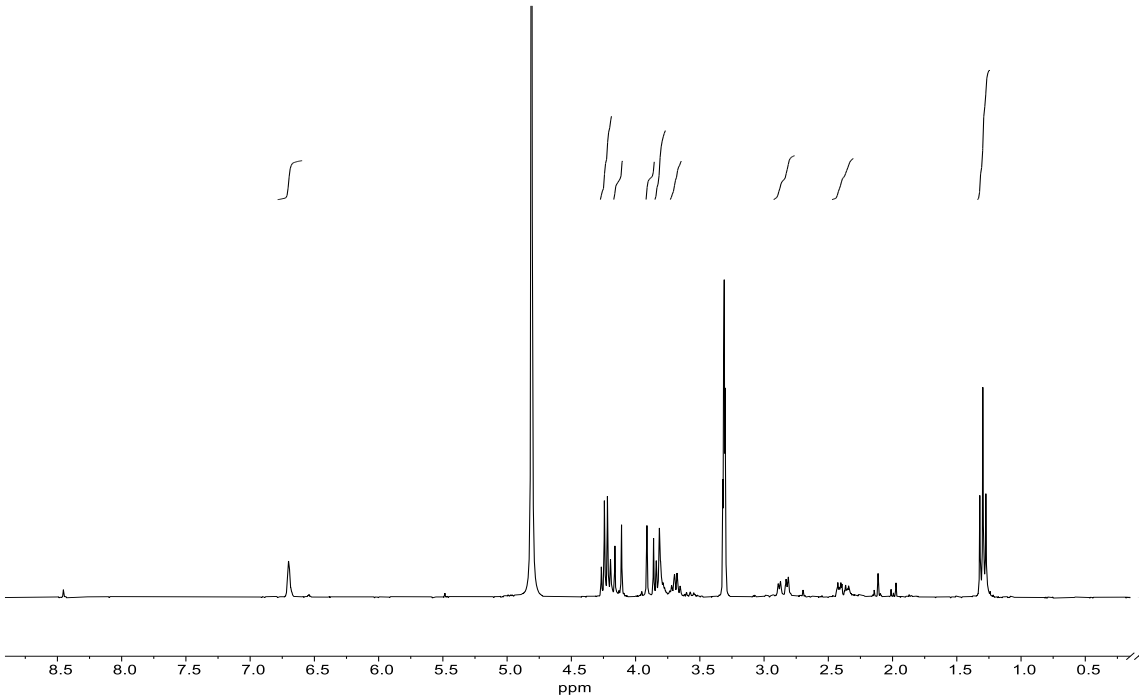
8.5
8.0
7.5
7.0
6.5
6.0
5.5
5.0
4.5
4.0
3.5
3.0
2.5
2.0
1.5
1.0
0.5
ppm

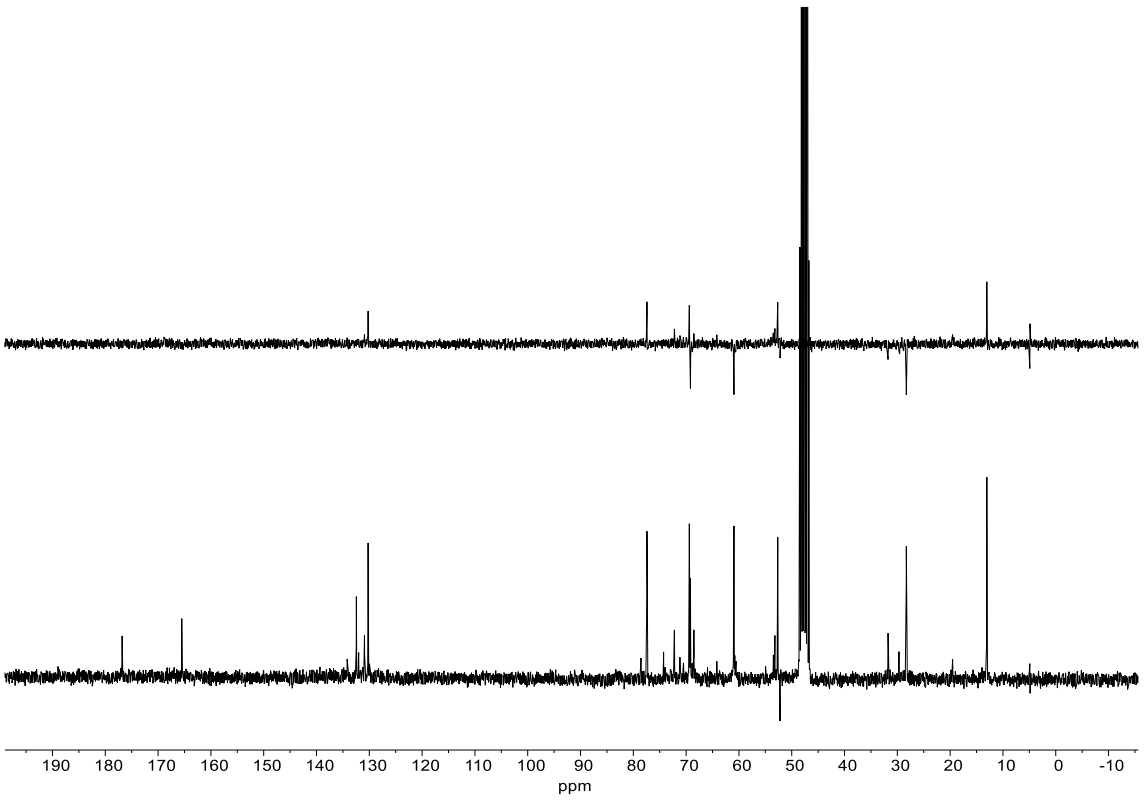
190
180
170
160
150
140
130
120
110
100
90
80
70
60
50
40
30
20
10
0
-10
ppm

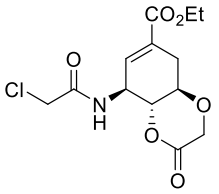
CO2Et
O
Cl
N
H
O
O
O

28

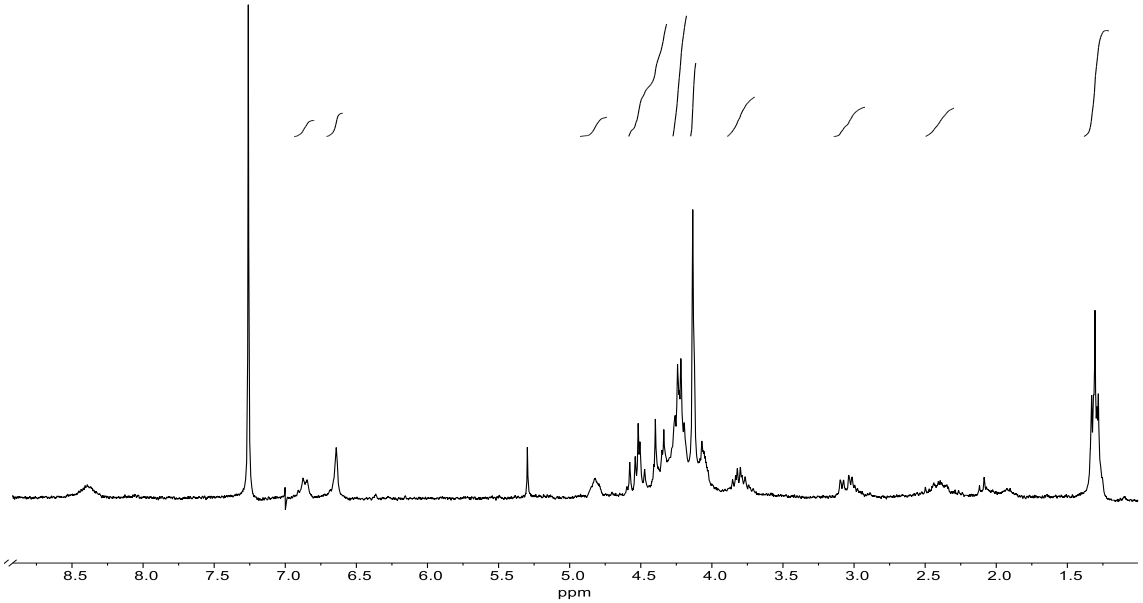
8.5
8.0
7.5
7.0
6.5
6.0
5.5
5.0
4.5
4.0
3.5
3.0
2.5
2.0
1.5
ppm

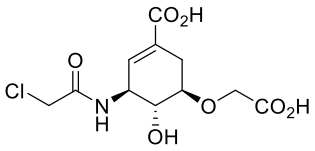
CO2H
O
Cl
N
H
O
CO2H
OH

19

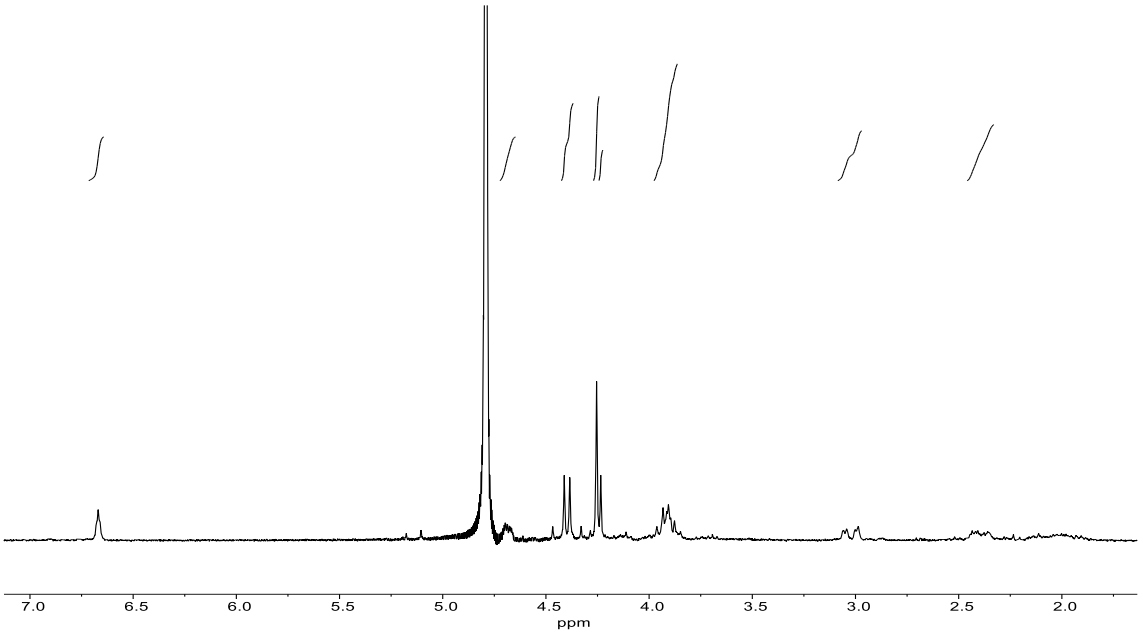
7.0
6.5
6.0
5.5
5.0
4.5
4.0
3.5
3.0
2.5
2.0
ppm